

On the study of kinematics of eruptive quiescent prominences observed in He 304 Å

Vishal Joshi¹ and Nandita Srivastava^{2*}

¹*Astronomy and Astrophysics Division, Physical Research Laboratory, Ahmedabad 380 009, India*

²*Udaipur Solar Observatory, Physical Research Laboratory, Udaipur 313 004, India*

Abstract. The observations taken in He 304 Å by the EIT telescope aboard SoHO reveals that these images are extremely useful in tracing prominences because of the relatively sharper spine which is better visible in 304 Å than in H $_{\alpha}$. We have developed a geometric technique of measuring the height of prominences. The technique was applied to six eruptive quiescent prominence images recorded by EIT in He 304 Å during January 2000–July 2003 in an attempt to identify the precursors of geo-effective coronal mass ejections (CMEs) that are associated with eruptive prominences. Our analyses show that prominence eruptions evolve through a pre-eruptive phase and an eruptive phase, which are characterized by lower velocities of several km s⁻¹ and eruptive velocities of several tens to hundreds of km s⁻¹, respectively. The analyses also show that during the pre-eruptive phase, a prominence rises at a constant acceleration of several cm s⁻² and not at constant velocity as reported by previous workers. We suggest that this phase is indicative of the precursor of prominence eruption. This might be useful in predicting the occurrence of an associated coronal mass ejection.

Keywords : Sun : prominences – Sun : coronal mass ejections (CMEs) – Sun : corona

1. Introduction

It is important to study the eruption of prominence with pre-eruptive stages in order to understand the basic processes occurring between magnetic field and coronal plasma. Eruptive prominences are often associated with CMEs. In particular, in the classical three

*e-mail:nandita@prl.res.in

part structured CMEs, the bright, compact central parts are believed to be the remnants of eruptive prominences (Crifo, Picat & Cailloux 1983; Sime, MacQueen & Hundhausen 1984; Hundhausen 1999). In fact, prominence activation and eruption can be used to understand the precursor or pre-eruptive phase of the associated CME. Therefore, a study of activation and eruption of prominences assumes importance in space weather study, too. Several studies have been made to understand the kinematics of eruptive prominence in the past. Most of these, were based on the studies of H_α images of the sun obtained from ground based telescopes. However, recently a few attempts have been made to study kinematics of eruptive prominences using SoHO EIT images, in particular the 304 Å images. Almost all these studies were limited to fast rise or eruptive stage of prominences. On the contrary, slow rise of prominence prior to its complete eruption is also important in order to understand the trigger mechanism of eruption which could be used to forecast the eruption of prominence. Pre-eruption slow-rise phases of quiescent filaments have been observed and reported earlier also (e.g., Tandberg-Hanssen et al. 1980). The slow rise of filaments/prominences is a common phenomena; but not universal (Kahler et al. 1988). For many filaments, therefore, the slow rise seems to be a critical feature of their evolution toward eruption. Earlier work suggests that when a slow rising prominence reaches a critical height it becomes unstable and erupts (Filippov & Den 2000, 2001). Therefore, an important parameter to predict its eruption is the height of prominence. In this paper, we studied the kinematics of selected eruptive prominences observed in He 304 Å, in particular the pre-eruptive slow rise phase of these prominences. We estimated critical height and velocity at which eruption occurs. Further, we derived the range of height in which eruptive prominences attain maximum acceleration and velocity. It is interesting to compare these heights with those of maximum acceleration of CME associated with the eruptive prominence to understand the driving mechanisms in each kind of phenomena.

2. Observational data

In the present study, we used the data-set of HeII 304 Å images take by EIT on SOHO which was launched in December 1995 (Delaboudiniere et al. 1995). In particular, the Extreme Ultraviolet Imaging Telescope (EIT), in continuous operation since early 1996, records images of the Sun in four selected emission lines: Fe IX(171 Å), Fe XII(195 Å), Fe XV(284 Å) and He II(304 Å). The last line has a formation temperature of about 80,000 K, and the other three between 1 and 2 million degrees. As mentioned above, H_α images have been traditionally used to study the kinematics of eruptive quiescent prominences due to availability of large data set from the ground. However, the most obvious advantage of using HeII 304Å images over H_α image is that the upper edge of prominence is more clearly pronounced in former compared to that in latter. This enables us to measure the height with better accuracy in HeII 304Å images. Usually EIT records images of the size 1024×1024 pixels. However, to reduce the size of the data sometimes image size is reduced to 512×512 pixels. As per the routine observation plan of the EIT telescope, only 3-4 images per day are taken in HeII 304 Å line. However a few times in a year,

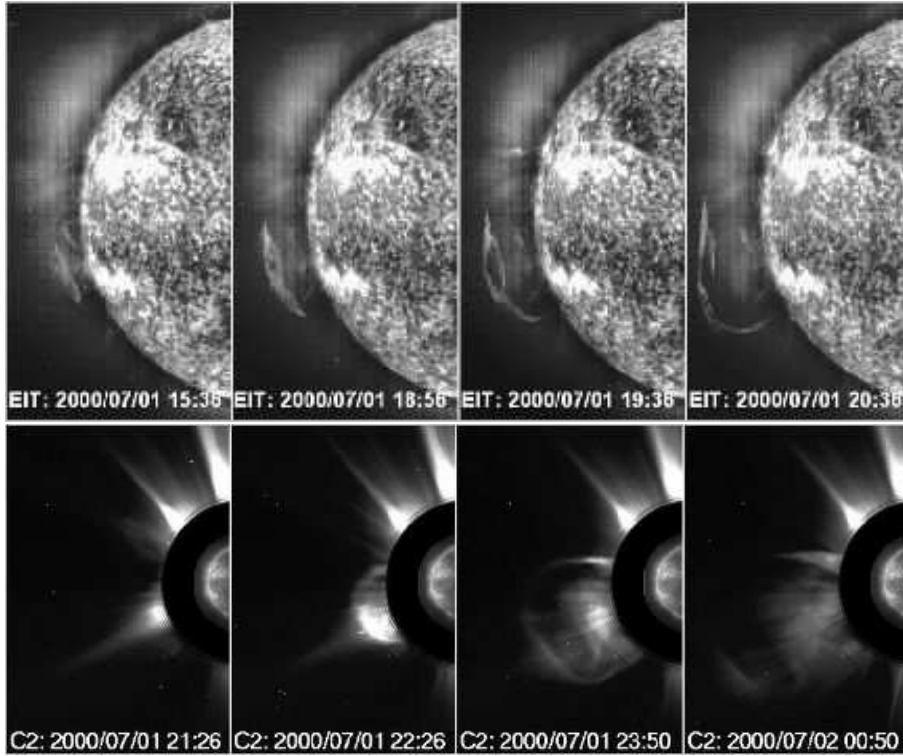


Figure 1. Time-lapse images of eruptive prominence observed in He 304 Å on July 1, 2000 (upper panel). The associated coronal mass ejection shows three part structure in LASCO-C2 white-light images (lower panel).

for several days, EIT images the full disk of the sun 5 times per hour in HeII 304Å line under ‘CME watch’ program. Sometimes, under ‘high-cadence’ observation campaign, images are recorded at even faster rate. For this study, we used images taken under either ‘CME watch’ or ‘high cadence’ observation to improve the temporal resolution. These images are recorded in FITS format and are downloaded from SoHO EIT online archive available at <http://umbra.nascom.nasa.gov/eit/eit-catalog.html>. For the present study, we selected a data-set comprising of high cadence images (3-12 frames per hour) obtained in HeII 304 Å and LASCO-C2 images. Six events of near limb eruptive quiescent prominences and associated CMEs were chosen out of this data-set.

3. Data analysis technique

When the prominences are on the limb, it is reasonably easier to measure its height and a better estimate of the true height is obtained. However, the difficulty arises in measuring

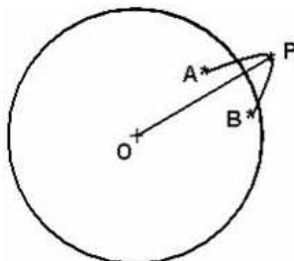


Figure 2. Sketch of the coordinates of the footpoints, A and B of the prominence when they both lie inside the disk. Here O denotes the origin of the centre of the coordinate system and P denotes the highest point of the prominence.

the height of a prominence when it is not on the limb but one of its foot point or the entire prominence is inside the disk. On the basis of some assumptions, we developed an algorithm to measure the height of prominence when it is inside the disk and not close to the disk-center. We used IDL programming language to program the technique used for measurement.

3.1 Prominence height measurement algorithm

If both foot points of prominence are behind the solar limb, we assume that the measured projected height of the prominence is the true height of the prominence. In the case, in which one or both foot points are inside the solar disk, a method to estimate the true height of such prominence is described in this section. We assume that

1. a prominence is a linear structure on solar surface,
2. foot points of a prominence lie on the surface of the sun,
3. a prominence rises normal to the surface of the sun.

To find the height, a 3-dimensional coordinate system is defined. In this coordinate system, the centre of the sun is at the origin, east-west direction is X axis, with west being in the positive direction and north-south direction is Y axis with center to north being the positive direction. Z axis is in the direction of line-of-sight.

Therefore, the equation of solar sphere becomes

$$x^2 + y^2 + z^2 = R^2 \quad (1)$$

The two dimensional image can be treated as a projection of the three dimensional space on X-Y plane. One can obtain directly the x and y coordinates of any point from an image. If one can obtain z coordinate of any point on the prominence, then all the three coordinates of that point can be obtained and hence the height can be calculated using equation (1). In order to calculate z coordinate of any point lying on the prominence, we calculated z coordinate of foot points. Suppose the foot points of prominence are A (x_A, y_A, z_A) and B (x_B, y_B, z_B) where x_A, y_A and x_B, y_B are known directly from image. As per our assumption, A and B are on the solar surface and hence satisfy equation (1). Therefore, z coordinates of both foot points are given by

$$z_i = \sqrt{R_0^2 - x_i^2 - y_i^2} \quad (2)$$

where $i = A, B$. Hence equation of plane passing through points O(0,0,0), A(x_A, y_A, z_A) and B(x_B, y_B, z_B) and normal to the surface of the sun is given by

$$z = ax + by \quad (3)$$

where constants a and b are given by the following equations. As per our assumption the erupting prominence always lies on this plane.

$$a = \frac{z_A y_B - y_A z_B}{x_A y_B - y_A x_B} \quad (4)$$

and

$$b = \frac{x_A z_B - z_A x_B}{x_A y_B - y_A x_B} \quad (5)$$

Now any point P (x_P, y_P, z_P) on the prominence must satisfy the equation of plane (2). The coordinates of the point P (x_P, y_P) can be obtained from image and z_P can be calculated from eq. (2) and is given by

$$z = ax_P + by_P \quad (6)$$

And height of P is given by

$$h_P = \sqrt{(x_P^2 + y_P^2 + z_P^2) - R_0^2} \quad (7)$$

Now we have all the coordinates of points O, A and B, therefore the equation of a plane passing through these three points can be obtained. This plane is normal to the surface of the sun on great circle passing through A and B and hence, by our assumption, erupting prominence always lies on this plane.

The heights of the leading edge of the prominence were estimated using the above technique at several instants. We further estimated the velocity and acceleration from the measured height and time values using 2 point running average for smoothing and 3 point interpolation method in height-time data before estimating the derivative for velocity using 3- point Lagrangian interpolation and derivative method.

Table 1. General Parameters for 6 erupting quiescent prominences.

Event No.	Date	Max. Vel. (Km s ⁻¹)	Height range (R _⊙) for max. Vel (km)	Max. Acc. (m s ⁻²)	Height range (R _⊙) for Max. Acc.
1	8 Jan 2000	62	0.48 -	25	0.39 - 0.42
2	8 Jan 2000	130	0.71 - 0.66	77	0.57 - 0.64
3	1 Jul 2000	22	0.45 -	3	0.24 - 0.29
4	25 Oct 2002	154	0.62 -	66	0.43 - 0.48
5	25 Oct 2002	38	0.32 - 0.34	17	0.31 - 0.33
6	30 Jul 2003	25	0.19 - 0.22	11	0.15 - 0.17

Table 2. Measured parameters for the slow rise phase of eruption of prominences.

Event no.	Date	acceleration (cm s ⁻²)	Time duration (Hours)	Maximum height (R _⊙)
1	8 Jan 2000	7.65	3.81	1.21
2	8 Jan 2000	7.21	8.10	1.12
3	1 Jul 2000	slow rise not observed		
4	25 Oct 2002	4.15	6.2	1.11
5	25 Oct 2002	4.77	1.2	1.04
6	30 Jul 2003	11.84	6.59	1.13

4. Conclusions

In this paper, we studied the kinematics of eruptive quiescent prominences observed in He 304Å. The following results were obtained from this study.

1. The eruption occurred in two distinct phases in the eruptive prominences studied here. During the initial phase, a slow rise - a general characteristic of all the events was observed. This phase is indicative of the precursor of prominence eruption. This might help to predict the occurrence of an associated coronal mass ejection.
2. The initial slow rise phase shows constant motion with an acceleration of 4 - 12 cm s⁻². This is in contrast to prior reports in which slow rise with constant velocity has been reported. (Tandberg-Hanssen et al. 1980; Sterling & Moore 2005).
3. In the second or the eruptive phase, prominences experience larger acceleration ranging between 10 and 80 m s⁻² achieving a velocity in the range 20-150 km s⁻¹. This range corresponds to that of the core of the CMEs (Table 1 & 3). These results have an important bearing on determining the onset time of CME occurrence. In fact, acceleration of prominences in eruptive phase is also observed in active

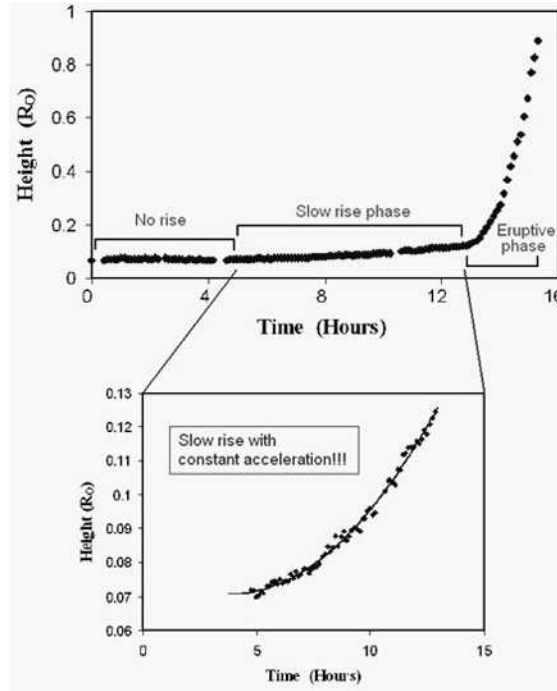


Figure 3. The height time plot of the event reveals two distinct phases. The first phase is marked by a slow or gradual rise for several hours and the second phase is marked by eruptive phase which reveals conspicuous acceleration. Lower panel shows the blow-up of the height time plot of the slow rise phase. The curve is fitted with a second order polynomial. Here the prominence clearly rises with acceleration of the order of 7.7 cm s^{-2} in contrast to prior studies which suggested a slow rise with constant velocity.

Table 3. Measured parameters for the associated CMEs.

Event		CME Leading edge		CME Core	
No.	Date	Vel. (km s^{-1})	Acc. (m s^{-2})	Vel. (km s^{-1})	Acc. (m s^{-2})
3	01 Jul 00	204	–	191	–
5	25 Oct 02	344	16.2	18	16.8

prominences associated with CMEs (Subramanian et al. 2003, Kundu et al. 2004). However, the long term slow rise for several hours as noted in the present analysis is typical of quiescent prominences.

4. Based on a study of H-alpha prominences, it has been shown that prominences with

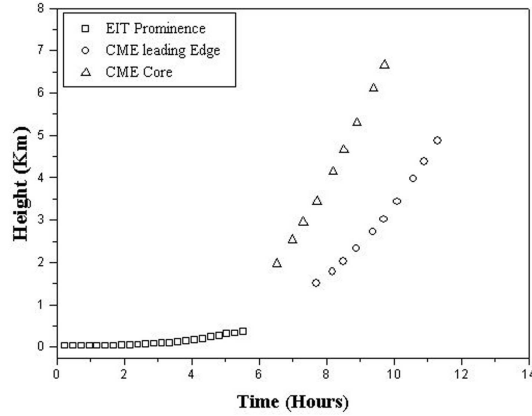


Figure 4. The height-time plot shows that the core of the CME corresponds to the prominence observed in He 304 images. The similarity in height-time profiles for the leading edge and the core of the CME suggest that same forces may be acting on both the features. This is crucial for understanding of the trigger mechanism of a CME associated with an eruptive prominence.

height $> 0.2 R_{\odot}$ have an associated CME (Gilbert et al. 2000). This is true for all but one case in our study. This implies that beyond $0.2 R_{\odot}$ forces driving for a prominence is same as that which drives a CME.

5. The average maximum height of eruptive prominences observed in H_{α} as reported by Gilbert et al. (2000) is $1.45 R_{\odot}$. This study reveals that the maximum height range may extend up to $2 R_{\odot}$. This suggests that EIT 304 Å images can be used to trace prominences up to higher altitude compared to H_{α} images. This is very helpful in identifying the prominence material with the three part structured CME observed usually in white light.

The high cadence data obtained in He 304 Å allows us to compare quiescent prominence eruption to a greater height than that observed in H_{α} . This study can be extended to understand the role of eruptive prominences in the associated CMEs. Criteria of eruption of prominences based on the measurable quantity like critical height and critical velocity of slow rise can also be estimated.

Acknowledgements

The authors thank the SOHO/EIT and LASCO consortia for providing the images used for analysis. SOHO is an international cooperation between ESA and NASA. One of the authors, NS acknowledges travel support as a Co-I on NSF Grant ATM-0519249 and helpful discussion with the research team including O. Engvold, Y. Lin, T.Forbes, Yu. Litvinenko, S.F. Martin, A. Pevtsov and K.S. Balasubramaniam.

References

- Crifo, F., Picat, J. P., & Cailloux, M., 1983, *SoPh*, 83, 143
Delaboudinière, J.P., Artzner, G.E., & Brunaud, J., et al., 1995, *SoPh*, 162, 291
Filippov, B.P. & Den, O.G., 2000, *AstL*, 26, 322
Filippov, B.P. & Den, O.G., 2001, *JGR*, 106, 25177
Hundhausen, A. J. 1999, *The Many Faces of the Sun : A Summary of the Results From NASA's Solar Maximum Mission*, eds K. T. Strong et al., New York: Springer - Verlag, 143
Kahler, S. W., Moore, R. L., Kane, S. R., & Zirin, H., 1988, *ApJ*, 328, 824
Kundu, M. R., White, S. M., Garaimov, V. I., Manoharan, P. K., Subramanian, P., Ananthakrishnan, S., & Janardhan, P., 2004, *ApJ*, 607, 530
Sime, D. G., Mac Queen, R. M., & Hundhausen, A. J., 1984, *JGR*, 89, 2113
Sterling, A., & Moore, R. M., 2005, *ApJ*, 630, 1148
Subramanian, P., Ananthakrishnan, S., Janardhan, P., Kundu, M. R., White, S. M., & Garaimov, V. I., 2003, *SoPh*, 218, 247
Tandberg - Hanssen, E., Martin, S. F., & Hansen, R. T., 1980, *SoPh*, 65, 357